Robotics and Autonomous Systems 115 (2019) 121–129

Contents lists available at ScienceDirect

Robotics and Autonomous Systems

journal homepage: www.elsevier.com/locate/robot

Shared control of a robotic arm using non-invasive brain–computer interface and computer vision guidance

Yang Xu, Cheng Ding, Xiaokang Shu, Kai Gui, Yulia Bezsudnova, Xinjun Sheng, Dingguo Zhang *

State Key Laboratory of Mechanical System and Vibration, School of Mechanical Engineering, Shanghai Jiao Tong University, 800 Dongchuan RD., Minhang District, Shanghai, China

ARTICLE INFO

Article history:
Received 21 July 2018
Received in revised form 2 January 2019
Accepted 20 February 2019
Available online 25 February 2019

Keywords:
Brain–computer interface
Motor imagery
Computer vision
Shared control
Robotic arm

ABSTRACT

Control of a robotic arm using a brain–computer interface (BCI) for reach and grasp activities is one of the most fascinating applications for some severely disabled people, which is especially challenging for the non-invasive BCIs based on electroencephalography (EEG). In this paper, shared control is applied to realize the control of a dexterous robotic arm with a motor imagery-based (MI-based) BCI and computer vision guidance. With the utilization of the shared control, the subjects just need to move the robotic arm by performing only two different mental tasks to the surrounding area of the target. The accurate pose of the target is estimated by a depth camera equipped in the robot system. Once the endpoint of the robotic arm enters the pre-defined vision-guided region, the robotic arm will grasp the target autonomously. Five healthy and inexperienced subjects participated in the online experiments and the average success rate is above 70% even with no specific user training. The results show that the shared control can make the robotic arm accomplish the complex tasks (reach and grasp) with the simple two-class MI-based BCIs.

1. Introduction

1.1. Robotic arm control with BCIs

Brain–computer interface (BCI) is a control and communication option between human and external devices, which does not depend on the peripheral nerves and muscles [1]. For people with paralysis due to trauma, stroke, etc, BCIs are conceived to hold promise for increasing self-sufficiency in their daily lives. In order to restore movement control in paralysed people, it has always been an ambitious goal to design a brain-actuated robotic arm for reach and grasp activities in a three-dimensional (3D) space.

Most advances in BCI-controlled robotic arms are achieved using invasive BCIs, which can acquire higher-quality of signals than that of non-invasive BCIs. Subjects have learned to control the robotic arm to perform complex functional tasks by decoding signals acquired by implanted electrodes [2–4]. However, the technical difficulties and clinical risks of the invasive BCIs remain the major limitations toward the practical applications. Additionally, ethical concerns exist widely among the invasive technologies [5].

In contrast, the non-invasive BCIs which record the electroencephalography (EEG) over the scalp are easier and safer. Previous studies have validated that human subjects could control the planar movement of a robotic arm using BCIs with three [6] or four [7] different mental tasks. Regarding more complex movement, a non-invasive BCI system using P300 potentials was developed to realize the control of a robotic arm with multiple degrees-of-freedom (DOFs) [8]. A main drawback with the evoked BCI is the requirement of external stimulus, which restricts its practical applications [5]. Moreover, subjects are required to look at a screen to elicit the evoked potentials during the control, which can distract them from observing the realtime state of the robotic arm [8]. It is preferable to use a non-invasive BCI extracting spontaneous features which does not depend on the external stimulus. A related research was reported recently, in which a motor imagery-based (MI-based) BCI was utilized to move a robotic arm in a 3D space [9]. The 3D movement was completed with a sequential movement strategy, which enabled the subjects to achieve the 3D movement by utilizing only four discriminative mental tasks. Despite of this, user training is required before the realtime control of the robotic arm. The subjects have to learn to generate four different mental states. Also, they need to adapt to the sequential movement strategy, which brings more cognitive burden.

In control of a dexterous robotic arm, one tremendous challenge is the limited capacity of the non-invasive BCIs based on spontaneous brain activities. The independent control commands

* Corresponding author.
E-mail address: dgzhang@sjtu.edu.cn (D. Zhang).

https://doi.org/10.1016/j.robot.2019.02.014
0921-8890/

generated from the non-invasive spontaneous BCIs are not sufficient to control a dexterous robotic arm. The most advanced one can just output three pairs of independent commands, which corresponds to six different mental tasks [10]. However, six or seven pairs of independent control commands are needed theoretically, if the open and close of the end gripper is included, to perform reach and grasp activities in a 3D space. Besides, intensive user training is required to master the usage of a spontaneous BCI even though there are just two [9,11] or three [10] pairs of independent commands, which brings more cognitive burden over the disabled users. Facing the practical applications in the daily life, as long as the functional activities can be achieved, it is preferable that the BCI system is simple enough and easy to use.

1.2. Shared control

Shared control can be a solution for the problem of limited capacity of non-invasive BCIs in control of a robotic arm with multiple DOFs. The intelligent device and the subject collaborate to control the whole system when shared control is used. By reducing the requirements of the BCIs, it may improve the usability of the BCI-controlled robotic arms in practice. This control strategy has been applied in some brain-actuated applications to enhance the performance of the systems, including wheelchair [12,13] and helicopter [14].

In case of robotic arm control, shared control strategy has been used to improve the grasping performance (e.g., the adjustment of the gripper orientation to grasp the target accurately) for the invasive BCIs while the 3D movement of the robotic arm is under control of the subjects [15–17]. However, it is still difficult now for the spontaneous non-invasive BCIs to finish the 3D movement. The number of output commands is limited because of the poor quality of the EEG signals recorded from the scalp. Although it was demonstrated that people can learn to move the cursor in a virtual 3D space through a spontaneous non-invasive BCI by producing three pairs of independent control commands [10], long-term user training is required and the system has not been verified with a real robotic arm yet. Thus, with the shared control, should not only the realization of steady grasping function be considered for the spontaneous non-invasive BCIs, the possibility of performing 3D movement with less than three pairs of independent control commands is also worthy of exploration. If less independent commands are required, the output accuracy of the BCI system holds the potential to be higher [18,19]. In addition, it may also decrease the time of user training before use, which will help a lot in applying the spontaneous non-invasive BCIs in the daily life.

In the present study, we apply a shared control strategy to an MI-based BCI for reach and grasp tasks in a 3D space. Due to the introduction of machine autonomy, only binary output from the BCI is required during the tasks, which makes the potential of this system extend beyond a laboratory study.

2. Methods

The architecture of this shared control system is diagrammed in Fig. 1. The whole system consisted of three subsystems: the BCI system, the robot system and the arbitrator. The output of the BCI system was two types of control commands following the EEG signals acquisition and decoding. The robotic arm could move in a horizontal plane under the BCI-guided control. In the robot system, the pose of the target block was estimated after the point clouds were captured by a depth camera fixed at one corner of the table. The robotic arm could then plan and execute the motion to grasp the target block once under the vision-guided control. The arbitrator defined the switch conditions between the BCI-guided control and vision-guided control according to the distance between the endpoint of the robotic arm and the target block.

2.1. BCI system

The BCI system ran on a Windows operating system. EEG signals were recorded using a 32 channel electrode cap and amplified by a BrainAmp amplifier (Brain Products GmbH, Germany). The sampling rate was 200 Hz. The subjects were asked to imagine the right- and left-hand movement to generate the two different mental states, which means the output of the BCI system was one pair of control commands.

Following the signal acquisition, a band-pass filter with a bandwidth of 8–30 Hz was utilized to obtain the mu and beta rhythms, which are considered to be correlated with MI tasks [20]. The common spatial pattern (CSP) algorithm was implemented to extract the signal features [21]. The extracted features were classified by a linear discriminant analysis (LDA) classifier. The binary output of the LDA classifier was sent out through a serial communication module. The analysis time window was set to be 1 s with a step length of 0.5 s.

A training session was implemented to obtain the parameters of the LDA classifier before online control. It is different from the user training, which is used to indicate the process of learning to finish the specific tasks (e.g., how to transfer from 1D control to 2D control [11]). The training session consisted of 60 single trials. Half of these trials were right-hand MI tasks and the others were left-hand MI tasks. The subjects imagined the corresponding hand movement according to the visual cues shown in a random order on the screen. The training session for each subject lasted for about 10 min. After the training session, the subjects could then generate two types of BCI control commands to move the robotic arm online.

2.2. Robot system

A UR5 robot (Universal Robots A/S, Denmark) with six DOFs was employed in the experiments. The maximum working radius of the robot is 0.85 m. A RG2 gripper (On Robot ApS, Denmark) was equipped at the end of the robot. The working stroke of the gripper is 0.11 m. The robot system ran on a Ubuntu and ROS operating system. Generally, this subsystem realized three functions: pose estimation, BCI-guided control and vision-guided control.

2.2.1. Pose estimation

The pose of the target block was estimated through the iterative closest point (ICP) algorithm. A RealSense SR300 RGB-D camera (Intel Corporation, USA) was chosen to capture the point clouds of the working space. The camera was fixed at one corner of the table (Fig. 1). The height of the camera from the table was around 0.3 m. The acquired point clouds were firstly downsampled with a voxel grid filter. A passthrough filter was then utilized to cut the point clouds at the edge of scene. It is helpful to remove some outliers and get a clean surface with the target block on it. The point clouds of the target block were extracted by segmenting the point clouds of the table plane. To improve the quality of the final point clouds of the target block, a statistical removal filter was used. After the pre-processing, the ICP algorithm was applied to estimate the pose of the target block. The point clouds of the model were drawn manually according to the geometrical shape of the target block. The target block is made of wood and the length of it is 0.05 m.

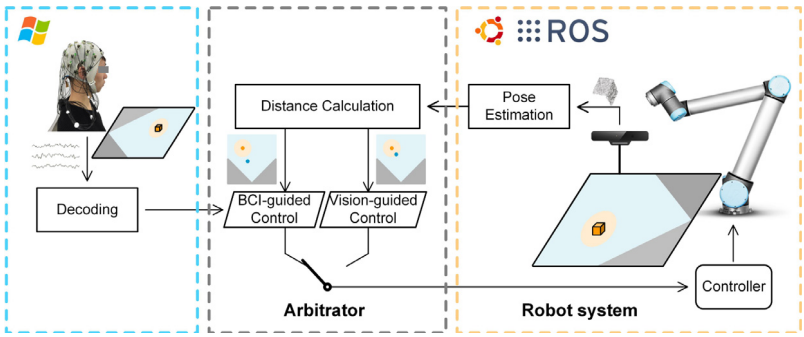

Fig. 1. Architecture of the shared control system. The whole system consisted of three subsystems: the BCI system (blue box), the robot system (orange box) and the arbitrator (gray box). After the EEG signals acquisition and decoding, the binary output of the BCI system was designed to move the robotic arm in a horizontal plane. In the robot system, the point clouds of the target block were captured by a depth camera fixed at one corner of the table. The pose of the target block could be estimated then. The robotic arm could plan and execute the motion to grasp the target block once under the vision-guided control. The switch conditions between the BCI-guided control and vision-guided control were defined by the arbitrator according to the distance between the endpoint of the robotic arm and the target block . (For interpretation of the references to color in this figure legend, the reader is referred to the web version of this article.)

2.2.2. BCI-guided control

During the BCI-guided control, when the classification result was right-hand MI, the endpoint of the robotic arm would go right front. Conversely, it would go left front. The degree between the movement direction and the front was 45 degrees. Therefore, the available reaching area was a sector in front of the subject, the central angle of which was 90 degrees [Fig. 2(b)]. This method enabled the endpoint of the robotic arm to move in a horizontal plane with just two types of control commands. A similar one has been successfully utilized in the wheelchair control based on an MI-based BCI [22].

The UR5 robot was controlled at the Script Level through the URScript programming language. The two different BCI control commands corresponded to two URScript commands: left front movement and right front movement. The endpoint of the robotic arm moved at a constant speed of 0.028 m/s in both conditions. The URScript commands were sent to the robot by a socket connection.

2.2.3. Vision-guided control

When the robot was under the vision-guided control, the final reach and grasp process was divided into three steps. Firstly, the endpoint of the robot would move to the right top of the target block. The wrist 3 joint of the UR5 robot then rotated for an appropriate angle to align the gripper to the target block. In the end, the gripper closed and grasped the target block for the subject. In this autonomous mode, the robot moved at the full speed.

2.3. Arbitrator

Fig. 2 shows the principles of the arbitrator. The front space of the robotic arm was divided into three parts: BCI-guided region, vision-guided region and the blind zone. The robotic arm was under control of the subject when the endpoint of the robotic arm located in the BCI-guided region. The robotic arm would take over once its endpoint entered the vision-guided region.

Because of the BCI control strategy, there were two blind zones in the two sides of the start point. However, the blind zones changed dynamically with the location of the start point. Now that the BCI system could only generate two different control commands and realize the planar movement, the robot itself should be able to adapt the height. Therefore, the shape of vision-guided region in our study was designed to be a cylinder around the target block and it did not have the limit in the z direction [Fig. 2(a)]. In that case, even the endpoint of the robotic arm could just move in the x–y plane under the BCI-guided control, it was still possible for the endpoint to go into the vision-guided region. The distance between the endpoint of the robotic arm and the target block was calculated in the x–y plane. The formula to calculate the distance goes as follows:

$$D = \sqrt{(x_R - x_B)^2 + (y_R - y_B)^2} \tag{1}$$

where D is the distance between the endpoint of the robot and the target block. x_R and y_R are the realtime locations of the endpoint of the robot. Similarly, x_B and y_B show the estimated locations of the target block. The coordinate system is shown in Fig. 2(a). T is determined to be the radius of the vision-guided region. In this experiment, T was set to be 0.1 m. To determine whether the control belongs to the subject or the robotic arm itself, a shared control strategy is computed with the following equation:

$$V = (1 - \alpha)V_S + \alpha V_R \tag{2}$$

where V is the final velocity command sent to the controller, V_S and V_R are the velocity commands generated by the subject and the robotic arm respectively. α is equal to 0 when $D > T$ while it changes to be 1 when $D < T$. Specifically, if $D > T$, it indicates the endpoint of the robotic arm is out of the vision-guided region, the robot is under the control of BCI. Vice versa, the robot itself will reach and grasp the target block autonomously with the guidance of vision.

During the online control of the robotic arm, the arbitrator was calculating the distance between the endpoint of the robot and the target block in realtime, making decisions if it should turn the mode switch from the BCI-guided control to the vision-guided control. Once the robotic arm entered the vision-guided region, the subjects could also notice that because the robotic arm moved faster under the vision-guided control.

2.4. Experimental paradigm

Eleven healthy subjects (9 males, 2 females, aged 24–30, mean age of 26 years old) were recruited in our experiment. Informed consent from every subject was given before the experiment. None of the subjects had the previous experience of realtime control with the MI-based BCI and six of them were naive BCI users. The study satisfies the Declaration of Helsinki. Before the online experiment, offline accuracy was calculated with the 5-fold cross validation. The data used for calculation was recorded in the training session. The offline accuracy of each subject is shown in Table 1. Since all of the eleven subjects had no previous experience of online control, before the robotic arm control experiment,

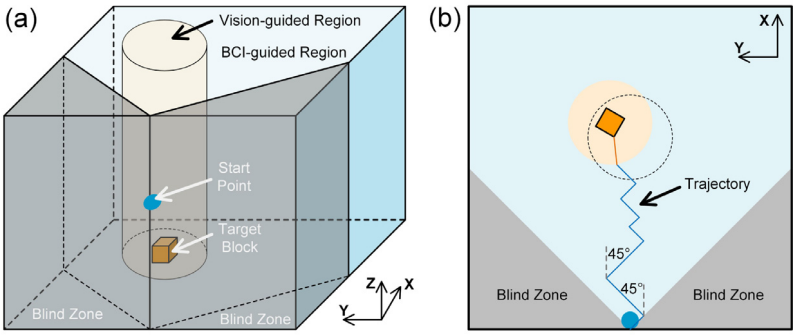

Fig. 2. Principles of the arbitrator. (a) Stereogram. The front space of the UR5 robot was divided into three parts: BCI-guided region (blue), vision-guided region (orange) and the blind zone (gray). The robotic arm was under control of the subject when the endpoint of the robotic arm located in the BCI-guided region. The robotic arm would take over once its endpoint entered the vision-guided region. (b) Top view. The polyline between the start point and the target block is a sample of trajectory. The circle drawn by dashed line indicates the area where the target block was placed during the online experiments. (For interpretation of the references to color in this figure legend, the reader is referred to the web version of this article.)

all of them were invited to participate in the preliminary experiment of online cursor control (5–10 trials) and they were not told about their offline accuracy. After that, they were asked if they wanted to continue with the following robotic arm control. As a result, six of them would feel frustrated easily during the preliminary experiment. They found it hard to control the cursor and gave up the following robotic arm control experiment. In the end, only five subjects finished the following online robotic arm control experiment. Offline analysis showed the BCI accuracy of the five subjects who took part in the robotic arm control experiment was higher than 80%.

The whole online experiments consisted of three sessions and each session lasted for no more than two hours, including the rest time. Each subject finished the whole experiments in three times. One session was completed in each time. In the first session, the subjects were required to finish the reach and grasp tasks in which the target blocks were located at eight fixed locations. As shown in Fig. 3(a), the eight fixed locations (L1–L8) were evenly distributed around a circle. The orientation of the eight target blocks was different. The location of the circle center was right in front of the start point at a distance of 0.4 m [Fig. 2(b)]. Considering the effective depth distance of the RGB-D camera, radius of the circle was set to be 0.1 m. In each trial, only one target block would appear in one of the eight chosen locations. The subject was then asked to control the robotic arm to reach and grasp the target block. For each location, the subjects were required to finish eight single trials. As a result, each subject should finish sixty-four single trials in session 1.

Once the endpoint of the robotic arm moved past the target block, the current trial would be judged to be a failure. Apart from this, the trial should also be considered as a failure if the robotic arm did not grasp the target block successfully when the system was under the vision-guided control. For the successful trials, the completion time and the trajectories of the endpoint of the robot were recorded. Apart from this, the trajectory efficiency (TE) of the trajectories was calculated. The TE is defined as follows:

$$TE = Tra_1/Tra_0 \tag{3}$$

where Tra_1 is the length of the trajectory. Tra_0 is the linear distance between the start point and the center of the target block. Smaller values of TE indicate more optimized trajectories.

In session 2, sixty-four random locations were generated inside the circle which was the same as that in session 1 [Fig. 3(b)]. In each trial, there was only one target block located inside the circle. Then the subject was asked to move the robotic arm to finish the reach and grasp task. The principle to determine the current trial to be a failure was same with that in session 1.

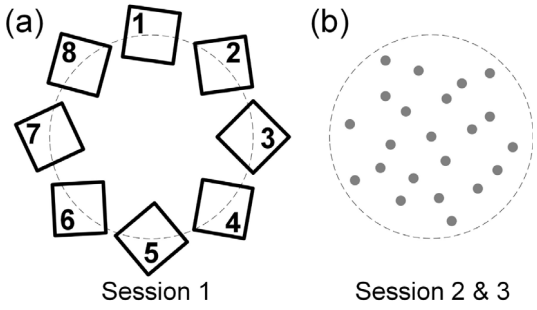

Fig. 3. Diagram of the target block locations. (a) The eight fixed locations (L1–L8) were evenly distributed around a circle in session 1. (b) In session 2 and 3, sixty-four random locations were generated inside the circle which was the same as that in session 1. The gray dots in the circle indicate the random locations.

Also, the completion time and the trajectories of the endpoint of the robotic arm were recorded. The subject needed to finish sixty-four single trials in this session.

Session 3 was designed to test the chance performance of the shared control system. In this session, the subjects sat still in the chair and looked at a blank screen instead of the robotic arm. At the same time, EEG signals were recorded from them to produce two random BCI control commands. The tasks required to finish were same with that in session 2. There were also sixty-four single trials in this session.

3. Results

All of the five subjects could finish the reach and grasp tasks in the experiment successfully. The scene of the online experiment is shown in Fig. 4. To evaluate the performance of the shared control system, the success rate was calculated and the completion time of the successful trials was recorded for each subject. Even with no specific user training, the average success rate of the five subjects was higher than 70%. Fig. 5 demonstrates the success rate and average completion time of the five subjects. The average success rate of the three sessions were 73.74%, 70.94% and 35.62% respectively. All the unsuccessful trials of the five subjects resulted from the bad BCI-guided control. Once the system was under the vision-guided control, the robotic arm could always finish the reach and grasp tasks successfully. It is partly because there was only one target in the workspace. Also, the workspace was clean and with no object occlusion. The session 3 was designed to examine the chance performance

Table 1
Offline accuracy of the eleven subjects with the MI-based BCI.

Subjects	A	B	C	D	E	F	G	H	I	J	K
Offline accuracy (%)	74.33 ± 5.4	65.51 ± 4.9	56.44 ± 9.9	84.67 ± 4.1	82.67 ± 5.7	87.44 ± 4.6	67.00 ± 6.9	97.33 ± 2.8	88.33 ± 4.7	76.56 ± 6.2	53.00 ± 6.3

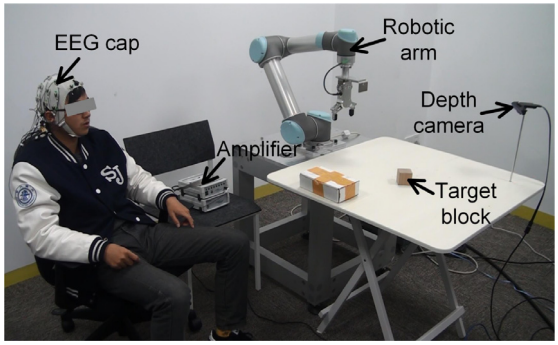

Fig. 4. Scene of the online experiment. The main components of the shared control system are indicated, including the EEG cap, the amplifier, the robotic arm, the depth camera and the target block.

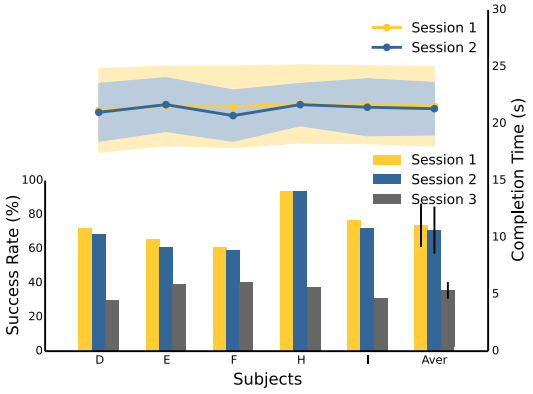

Fig. 5. Success rate and completion time. The bar chart shows the success rate of the session 1–3. Session 3 was completed with random EEG signals to check the chance performance. The line chart above shows the average completion time of session 1 and 2.

using the random EEG signals. The success rate of subject control was higher than the chance level. For the successful trials, the average completion time was 21.53 s in session 1 and 21.31 s in session 2. The average completion time was close across the five subjects mainly because the movement speed was constant and the distance required to cover during the tasks was similar. Moreover, the robotic arm would not move back and forth under the BCI-guided control because of the BCI control strategy (i.e., left front and right front movement), so the trajectory would not be more redundant. More specifically, the average completion time of each location in session 1 is shown in Fig. 6. Again, due to the constant movement speed and the BCI control strategy, the completion time of the same location across the subjects was close. The time of the nearer target blocks was less and the time of target blocks in symmetrical locations was similar. The average completion time of target blocks in L1 and L5 was 25.83 s and 16.99 s respectively. Although the mean time is similar, the performance of subject H is better among all the subjects. The standard deviation of the completion time for the subject is smaller compared with the other subjects, which indicates the subject had better control of the robotic arm during the online experiment. The subject also reported that the robotic arm could move as he wanted.

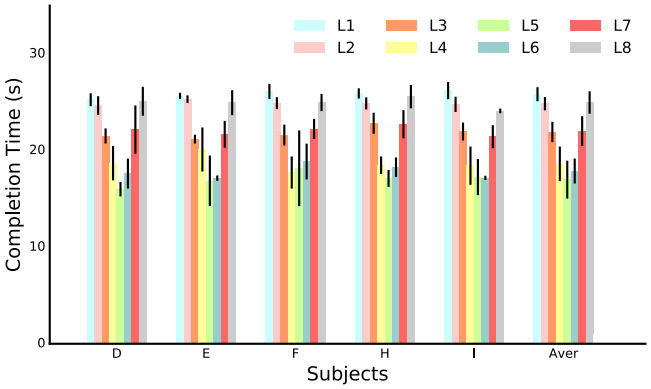

Fig. 6. Average completion time of each location in session 1. L1–L8 represents the eight locations which are shown in Fig. 3(a).

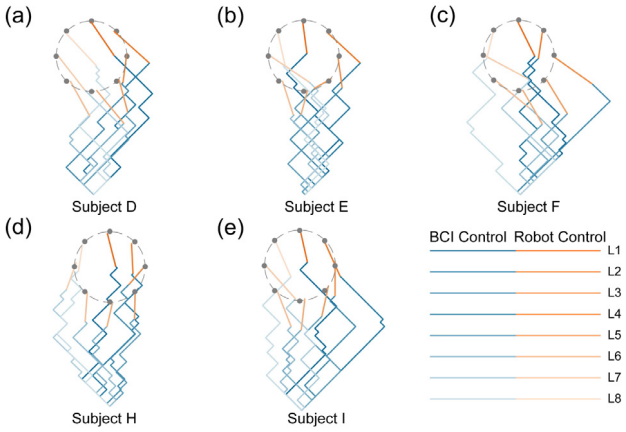

Fig. 7. Trajectory samples of the five subjects in session 1. For each location (L1–L8), the trajectory sample with median length is diagrammed. Blue lines indicate the BCI-guided control while the orange lines indicate the vision-guided control . (For interpretation of the references to color in this figure legend, the reader is referred to the web version of this article.)

In order to demonstrate more details of the online control, trajectories of the endpoint of the robotic arm were recorded. Fig. 7 shows the trajectory samples of the five subjects in session 1. For each location (L1–L8), the trajectory sample with median trajectory length is shown. Blue lines indicate the BCI-guided control while the orange lines indicate the vision-guided control. As is shown in Fig. 7, the robotic arm would only move in the left front and right front direction under the BCI-guided control. This does not bring more redundancy to the trajectory. Indeed, the length of the trajectory is mainly determined by where the robotic arm enters the vision-guided region. Beside the recorded actual trajectory samples, the TE of the trajectories was calculated. The average TE of each location in session 1 is diagrammed in Fig. 8. Generally, the value of TE is close to 1.4 in that the degree between the movement direction and the front was 45 degrees. From the average TE of eight locations, we can also find that the online performance of subject H is better among all the subjects because the TE is more steady.

The result distribution of the trials in session 2 and 3 is diagrammed in Fig. 9. All the trials of the five subjects are pooled

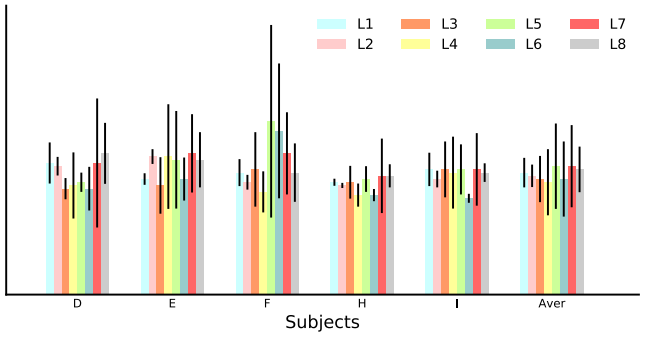

Fig. 8. The average TE of eight fixed locations in session 1. L1–L8 represents the eight locations which are shown in Fig. 3(a).

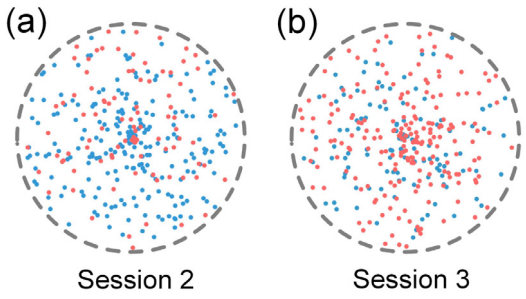

Fig. 9. The result distribution of all the trials in session 2 and 3. The blue dots indicate the successful trials and the red dots are the trials which are unsuccessful . (For interpretation of the references to color in this figure legend, the reader is referred to the web version of this article.)

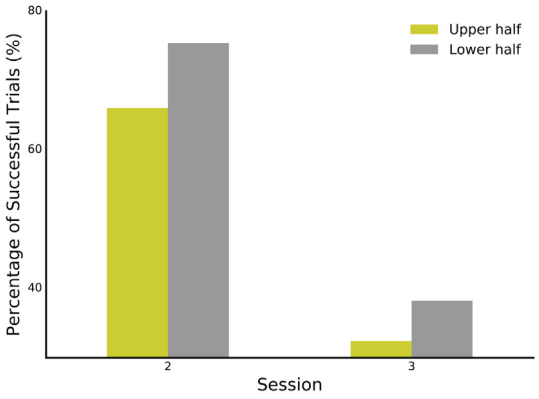

Fig. 10. The percentage of successful trials both in the upper and lower half of the circle in which the target blocks were located. The bar chart shows the result of session 2 and 3.

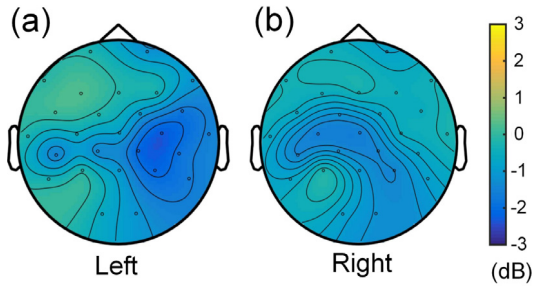

Fig. 11. Average topographical maps of ERD from subject H under the BCI-guided control. (a) Left-hand MI. (b) Right-hand MI.

together. It is found that the number of unsuccessful trials in the farther region is more than that in the nearer region after the initial analysis. To show the difference clearly, the circle in which the target blocks were located is divided into two parts: upper half and lower half (i.e., the target blocks which were located above the L3 and L7 shown in Fig. 3(a) belong to the upper half). For each part in session 2 and 3, the percentage of successful trials among all the trials in the corresponding part is calculated, which is shown in Fig. 10. In session 2, the percentage of successful trials in lower half is 9.4% higher than that in upper half. Likewise, the percentage of successful trials in lower half is 5.8% higher in session 3. The result is reasonable in that the workspace is a sector in the horizontal plane, the shorter distance between the start point and the target block means the proportion of the vision-guided region is higher. The robotic arm can then have the control in more conditions and the robotic arm could always finish the reach and grasp tasks in the online experiment when the system was under the vision-guided control. Apart from this, the subjects are more likely to become tired during a longer online control.

Fig. 11 shows the average topographical maps of event related desynchronization (ERD) from subject H during the BCI-guided control. When he was asked to do left/right hand MI and move the robotic arm to the left/right front, ERD can been seen in the right/left sensorimotor cortex.

4. Discussion

Because of the poor quality of EEG signals, control of a dexterous robotic arm for complex tasks is still hard only through the MI-based BCI, which restricts the further application of this control and communication option. In this study, a shared control strategy is utilized to overcome the difficulties of the limited capacity of EEG signals. With the help of machine autonomy, five of the subjects finished the online experiments even with no specific user training. Moreover, the MI-based BCI they used in the experiment is just with binary output, which is easier to use.

Generally, offline accuracy directly affects the online performance. The offline accuracy of subject H is 97.33% and the success rate is up to 93.75%. Also, the trajectory is more steady. The subject said he could control the movement of the robotic arm as he wanted during the online experiment. We also find the state of the subjects plays an important role in the online experiments. Although the offline accuracy of the subject F is 87.44%, his online performance is not so satisfactory. We noticed the subject often tended to move and relax his body between the trials adjacent, which may change the EEG signals and then affect the performance of the next trial.

Machine autonomy is utilized in this work to solve the problem of low signal-to-noise ratio of the EEG signals. Indeed, researchers have also come up with some other methods (e.g., the hybrid BCI) to increase the number of output commands or improve the performance. However, part of the hybrid BCIs combine evoked BCIs with the non-evoked BCIs [23,24] or other evoked BCIs [25,26], which can introduce the disadvantages of the evoked BCIs (e.g., the distraction during the online control). Some other hybrid methods are based on the combination between EEG and electromyogram (EMG) [27,28] or eye gaze [29,30]. However, they are just available for the users who still own the residual muscular movement. For the 'locked in' disabled people, only the independent BCIs can be useful to them. The object of these hybrid approaches is to provide more input channels for the users so that the users can fully control the machine or the performance of the systems will be better. However, it can also bring more cognitive burden to the users during the use because the

combination of different interfaces might add more complexity to the system. Compared with the hybrid approaches, we believe the introduction of machine autonomy is a better solution. In our experiment, five of the subjects could finish the reach and grasp tasks only using a MI-based BCI with binary output, which is nearly the simplest MI-based BCI. Therefore, the usability of the shared control system may be more satisfying and five of the subjects could finish the tasks even with no specific training. If the users can produce general high-level commands to represent their intention and be involved in the process only using a very simple MI-based BCI. And if the intelligent machine is able to infer the user intention and help the users with the low-level and detailed operation at the same time, it will be more user-friendly in the real applications.

Along with the shared control, kinematic control [3] and goal selection [30–36] are other two methods to operate the robots for functional tasks. For kinematic control, the subject needs to specify the exact movement of the device through a BCI [37]. In order to control a robotic arm with six DOFs, the user has to produce six pairs of independent commands. For goal selection, the subject only needs to select a functional option (e.g., drinking water) and the device finishes all the detailed movement autonomously [37]. Kinematic control is flexible but it requires more control commands, which is not suitable now for the MI-based BCIs to achieve 3D movement and some other complex functional tasks. Even though the human subjects can learn to output so many different kinds of control commands, intensive training is required before use, which makes the system harder to use. In addition, it should be hard for the BCI control to complete some accurate operations (e.g., aligning the gripper to the target in order to grasp it) while one of the advantages of the autonomous control is the higher position accuracy. Goal selection is more simple while all the operations are required to be fully defined previously, so it may not be applied in a flexible way. Shared control is a good combination of the above two methods. In a shared control system, users may have the control throughout the task at a high level with freedom to represent their intention. In the other hand, the intelligent machine helps with the low level and detailed movement accurately. Moreover, with the assistance of machine autonomy, the users can finish the complex functional tasks just with a simple BCI. In our case, the MI-based BCI we used is a simple one only with the binary output. Compared with goal selection, users are allowed to have unconstrained movements and make use of the system in a more flexible way. More user involvement in the operation process is also beneficial to the system safety. The outside environment is evolving and there might be unpredictable events. Even though the machine is becoming more and more intelligent now, it is still hard for the machine to deal with all different conditions appropriately. Human users have better sensing capabilities, they can make correct decisions in advance and intervene the movement of machine. In addition, more user involvement is helpful to increase the sense of agency [38]. It is preferred to reserve some control of the machine for the disabled people [39].

There are also some limitations in the current work. Firstly, the subjects could just move the robotic arm forward in the horizontal plane with the binary output BCI. If the subject wants to place the target back to himself, the system cannot fulfill the requirement. Recently, a new protocol was reported in which subjects could move the cursor to any location in a plane using a BCI with only binary output [40]. This approach is suitable to be integrated in our system. Secondly, only the task performance was analyzed in the current research and the user experience was not evaluated quantitatively. Since the whole system is initially designed for people with paralysis, standardized tests of their user experience (e.g. user acceptance and perceived difficulty) should be conducted [16] to evaluate the usability of the system more thoroughly. Apart from this, although eleven subjects were recruited in our research, only five of them the accuracy of whom was relatively high finally completed the online robotic arm control experiment. The results indicate that the current shared control strategy is not able to assist the disabled people whose BCI accuracy is low. The weight of machine autonomy may be increased or other better shared control strategies can be designed to help more potential users to use our system.

We are also trying to do some extra work in the future to improve our system further and expand the shared control strategy to more complex scenarios. First of all, a new seamless and parallel shared control strategy is preferred. For the present, the whole process of reach and grasp is divided into two serial phases discretely: BCI-guided control and vision guided control. The control option between the subject and the robotic arm is determined through a binary switch. It should be better if the subject is able to control the robotic arm all the time with a simple BCI at a high level (e.g., gross movement and intension expression). Meanwhile, the intelligent robotic arm is assisting with the task potentially at a low level (e.g., aligning the gripper with the target accurately). Another prospective work is to combine the current robotic arm with a wheelchair. In the current system, the subjects now can only sit at a fixed location to finish the reach and grasp tasks. In the future, we can fix the robotic arm on a wheelchair to construct a mobile manipulation system so that the system can be applied in broader scenarios. Apart from the assistive technology, the shared control strategy may also be applied in rehabilitation, which is also an evolving field [41]. Currently, gross movement training is more common in rehabilitation [35,42–44]. If the machine autonomy is introduced, then the subjects can also participate in some more complex functional tasks (e.g. reach and grasp). In addition, a more advanced algorithm for multiple objects recognition and pose estimation will be studied. The new algorithm is also required to be tested in the cluttered environment where the system is designed initially to be applied in real life.

5. Conclusions

In this paper, a shared control strategy, which combines BCI control with computer vision guidance, is utilized to realize the control of a dexterous robotic arm for reach and grasp activities in a 3D space. With the assistance of the vision guidance, the simple two-class MI-based BCI is sufficient. The simplification of BCI makes the system easier to use. The subjects finish the reach and grasp tasks even with no specific user training. In the future, the collaboration between human beings and intelligent machines holds promise to bring some real applications and assist disabled people in their daily lives.

Acknowledgments

This work is supported by the National Natural Science Foundation of China (No. 61761166006, No. 91848112), and the Shanghai Municipal Commission of Health and Family Planning (No. 2017ZZ01006). The authors would like to thank all the subjects for the participation of the experiments and thank Jianjun Meng, Junkai Xu, Meng Wang, Guangye Li and Bin Zhang for the useful discussions.

Appendix A. Supplementary data

Supplementary material related to this article can be found online at https://doi.org/10.1016/j.robot.2019.02.014.

References

[1] J.R. Wolpaw, N. Birbaumer, D.J. McFarland, G. Pfurtscheller, T.M. Vaughan, Brain–computer interfaces for communication and control, Clin. Neurophysiol. 113 (6) (2002) 767–791.

[2] L.R. Hochberg, D. Bacher, B. Jarosiewicz, N.Y. Masse, J.D. Simeral, J. Vogel, S. Haddadin, J. Liu, S.S. Cash, P. van der Smagt, et al., Reach and grasp by people with tetraplegia using a neurally controlled robotic arm, Nature 485 (7398) (2012) 372.

[3] J.L. Collinger, B. Wodlinger, J.E. Downey, W. Wang, E.C. Tyler-Kabara, D.J. Weber, A.J. McMorland, M. Velliste, M.L. Boninger, A.B. Schwartz, High-performance neuroprosthetic control by an individual with tetraplegia, Lancet 381 (9866) (2013) 557–564.

[4] M.S. Fifer, S. Acharya, H.L. Benz, M. Mollazadeh, N.E. Crone, N.V. Thakor, Toward electrocorticographic control of a dexterous upper limb prosthesis: Building brain-machine interfaces, IEEE Pulse 3 (1) (2012) 38–42.

[5] J. DEL R. MILLÁN, P.W. Ferrez, F. Galán, E. Lew, R. Chavarriaga, Non-invasive brain-machine interaction, Int. J. Pattern Recognit. Artif. Intell. 22 (05) (2008) 959–972.

[6] E. Iáñez, J.M. Azorín, A. Úbeda, J.M. Ferrández, E. Fernández, Mental tasks-based brain–robot interface, Robot. Auton. Syst. 58 (12) (2010) 1238–1245.

[7] E. Hortal, D. Planelles, A. Costa, E. Iáñez, A. Úbeda, J.M. Azorín, E. Fernández, Svm-based brain–machine interface for controlling a robot arm through four mental tasks, Neurocomputing 151 (2015) 116–121.

[8] M. Palankar, K.J. De Laurentis, R. Alqasemi, E. Veras, R. Dubey, Y. Arbel, E. Donchin, Control of a 9-dof wheelchair-mounted robotic arm system using a p300 brain computer interface: Initial experiments, in: Robotics and Biomimetics, 2008. ROBIO 2008. IEEE International Conference on, IEEE, 2009, pp. 348–353.

[9] J. Meng, S. Zhang, A. Bekyo, J. Olsoe, B. Baxter, B. He, Noninvasive electroencephalogram based control of a robotic arm for reach and grasp tasks, Sci. Rep. 6 (2016) 38565.

[10] D.J. McFarland, W.A. Sarnacki, J.R. Wolpaw, Electroencephalographic (eeg) control of three-dimensional movement, J. Neural Eng. 7 (3) (2010) 036007.

[11] J.R. Wolpaw, D.J. McFarland, Control of a two-dimensional movement signal by a noninvasive brain-computer interface in humans, Proc. Natl. Acad. Sci. 101 (51) (2004) 17849–17854.

[12] J.d.R. Millán, F. Galán, D. Vanhooydonck, E. Lew, J. Philips, M. Nuttin, Asynchronous non-invasive brain-actuated control of an intelligent wheelchair, in: Engineering in Medicine and Biology Society, 2009. EMBC 2009. Annual International Conference of the IEEE, IEEE, 2009, pp. 3361–3364.

[13] X. Perrin, R. Chavarriaga, F. Colas, R. Siegwart, J.d.R. Millán, Brain-coupled interaction for semi-autonomous navigation of an assistive robot, Robot. Auton. Syst. 58 (12) (2010) 1246–1255.

[14] A.S. Royer, A.J. Doud, M.L. Rose, B. He, Eeg control of a virtual helicopter in 3-dimensional space using intelligent control strategies, IEEE Trans. Neural Syst. Rehabil. Eng. 18 (6) (2010) 581–589.

[15] K.D. Katyal, M.S. Johannes, S. Kellis, T. Aflalo, C. Klaes, T.G. McGee, M.P. Para, Y. Shi, B. Lee, K. Pejsa, et al., A collaborative bci approach to autonomous control of a prosthetic limb system, in: Systems, Man and Cybernetics (SMC), 2014 IEEE International Conference on, IEEE, 2014, pp. 1479–1482.

[16] J.E. Downey, J.M. Weiss, K. Muelling, A. Venkatraman, J.-S. Valois, M. Hebert, J.A. Bagnell, A.B. Schwartz, J.L. Collinger, Blending of brain-machine interface and vision-guided autonomous robotics improves neuroprosthetic arm performance during grasping, J. Neuroeng. Rehabil. 13 (1) (2016) 28.

[17] K. Muelling, A. Venkatraman, J.-S. Valois, J.E. Downey, J. Weiss, S. Javdani, M. Hebert, A.B. Schwartz, J.L. Collinger, J.A. Bagnell, Autonomy infused teleoperation with application to brain computer interface controlled manipulation, Auton. Robots 41 (6) (2017) 1401–1422.

[18] J.R. Millan, J. Mouriño, Asynchronous bci and local neural classifiers: an overview of the adaptive brain interface project, IEEE Trans. Neural Syst. Rehabil. Eng. 11 (2) (2003) 159–161.

[19] G. Müller-Putz, R. Scherer, C. Brunner, R. Leeb, G. Pfurtscheller, Better than random: a closer look on bci results, Int. J. Bioelectromagnetism 10 (EPFL-ARTICLE-164768) (2008) 52–55.

[20] G. Pfurtscheller, F.L. Da Silva, Event-related eeg/meg synchronization and desynchronization: basic principles, Clin. Neurophysiol. 110 (11) (1999) 1842–1857.

[21] B. Blankertz, R. Tomioka, S. Lemm, M. Kawanabe, K.-R. Muller, Optimizing spatial filters for robust eeg single-trial analysis, IEEE Signal Process. Mag. 25 (1) (2008) 41–56.

[22] K. Tanaka, K. Matsunaga, H.O. Wang, Electroencephalogram-based control of an electric wheelchair, IEEE Trans. Robot. 21 (4) (2005) 762–766.

[23] B.Z. Allison, C. Brunner, C. Altstätter, I.C. Wagner, S. Grissmann, C. Neuper, A hybrid erd/ssvep bci for continuous simultaneous two dimensional cursor control, J. Neurosci. Methods 209 (2) (2012) 299–307.

[24] G. Pfurtscheller, T. Solis-Escalante, R. Ortner, P. Linortner, G.R. Muller-Putz, Self-paced operation of an ssvep-based orthosis with and without an imagery-based brain switch: a feasibility study towards a hybrid bci, IEEE Trans. Neural Syst. Rehabil. Eng. 18 (4) (2010) 409–414.

[25] E. Yin, Z. Zhou, J. Jiang, F. Chen, Y. Liu, D. Hu, A novel hybrid bci speller based on the incorporation of ssvep into the p300 paradigm, J. Neural Eng. 10 (2) (2013) 026012.

[26] Y. Li, J. Pan, F. Wang, Z. Yu, A hybrid bci system combining p300 and ssvep and its application to wheelchair control, IEEE Trans. Biomed. Eng. 60 (11) (2013) 3156–3166.

[27] R. Leeb, H. Sagha, R. Chavarriaga, J. del R Millán, A hybrid brain–computer interface based on the fusion of electroencephalographic and electromyographic activities, J. Neural Eng. 8 (2) (2011) 025011.

[28] K. Lin, A. Cinetto, Y. Wang, X. Chen, S. Gao, X. Gao, An online hybrid bci system based on ssvep and emg, J. Neural Eng. 13 (2) (2016) 026020.

[29] T.O. Zander, M. Gaertner, C. Kothe, R. Vilimek, Combining eye gaze input with a brain–computer interface for touchless human–computer interaction, Int. J. Hum. Comput. Interact. 27 (1) (2010) 38–51.

[30] H. Zeng, Y. Wang, C. Wu, A. Song, J. Liu, P. Ji, B. Xu, L. Zhu, H. Li, P. Wen, Closed-loop hybrid gaze brain-machine interface based robotic arm control with augmented reality feedback, Front. Neurorobot. 11 (2017) 60.

[31] C.J. Bell, P. Shenoy, R. Chalodhorn, R.P. Rao, Control of a humanoid robot by a noninvasive brain–computer interface in humans, J. Neural Eng. 5 (2) (2008) 214.

[32] A. Athanasiou, G. Arfaras, N. Pandria, I. Xygonakis, N. Foroglou, A. Astaras, P.D. Bamidis, Wireless brain-robot interface: user perception and performance assessment of spinal cord injury patients, Wireless Commun. Mobile Comput. 2017 (2017).

[33] A.H. Do, P.T. Wang, C.E. King, S.N. Chun, Z. Nenadic, Brain-computer interface controlled robotic gait orthosis, J. Neuroeng. Rehabil. 10 (1) (2013) 111.

[34] A. Athanasiou, I. Xygonakis, N. Pandria, P. Kartsidis, G. Arfaras, K.R. Kavazidi, N. Foroglou, A. Astaras, P.D. Bamidis, Towards rehabilitation robotics: off-the-shelf bci control of anthropomorphic robotic arms, BioMed. Res. Int. 2017 (2017).

[35] K.K. Ang, C. Guan, K.S.G. Chua, B.T. Ang, C. Kuah, C. Wang, K.S. Phua, Z.Y. Chin, H. Zhang, A clinical study of motor imagery-based brain-computer interface for upper limb robotic rehabilitation, in: Engineering in Medicine and Biology Society, 2009. EMBC 2009. Annual International Conference of the IEEE, IEEE, 2009, pp. 5981–5984.

[36] J. Tang, Z. Zhou, A shared-control based bci system: For a robotic arm control, in: Electronics Instrumentation & Information Systems (EIIS), 2017 First International Conference on, IEEE, 2017, pp. 1–5.

[37] D.J. McFarland, J.R. Wolpaw, Brain-computer interface operation of robotic and prosthetic devices, Computer 41 (10) (2008).

[38] D.-J. Kim, R. Hazlett-Knudsen, H. Culver-Godfrey, G. Rucks, T. Cunningham, D. Portee, J. Bricout, Z. Wang, A. Behal, How autonomy impacts performance and satisfaction: results from a study with spinal cord injured subjects using an assistive robot, IEEE Trans. Syst. Man Cybern. A 42 (1) (2012) 2–14.

[39] S. Jain, A. Farshchiansadegh, A. Broad, F. Abdollahi, F. Mussa-Ivaldi, B. Argall, Assistive robotic manipulation through shared autonomy and a body-machine interface, in: IEEE... International Conference on Rehabilitation Robotics:[Proceedings], Vol. 2015, NIH Public Access, 2015, p. 526.

[40] B. Xia, L. Cao, O. Maysam, J. Li, H. Xie, C. Su, N. Birbaumer, A binary motor imagery tasks based brain-computer interface for two-dimensional movement control, J. Neural Eng. 14 (6) (2017) 066009.

[41] A. Gharabaghi, What turns assistive into restorative brain-machine interfaces? Front. Neurosci. 10 (2016) 456.

[42] F. Grimm, A. Walter, M. Spüler, G. Naros, W. Rosenstiel, A. Gharabaghi, Hybrid neuroprosthesis for the upper limb: combining brain-controlled neuromuscular stimulation with a multi-joint arm exoskeleton, Front. Neurosci. 10 (2016) 367.

[43] D. Brauchle, M. Vukelić, R. Bauer, A. Gharabaghi, Brain state-dependent robotic reaching movement with a multi-joint arm exoskeleton: combining brain-machine interfacing and robotic rehabilitation, Front. Hum. Neurosci. 9 (2015) 564.

[44] A. Frisoli, C. Procopio, C. Chisari, I. Creatini, L. Bonfiglio, M. Bergamasco, B. Rossi, M.C. Carboncini, Positive effects of robotic exoskeleton training of upper limb reaching movements after stroke, J. Neuroeng. Rehabil. 9 (1) (2012) 36.

Yang Xu received the B.S. degree in mechanical engineering from the Jilin University, China in 2015. He is currently pursuing the M.S. degree in mechatronic engineering at the Shanghai Jiao Tong University, China. His research interests include brain–computer interface, computer vision and shared control.

Cheng Ding received the B.S. degree in mechanical engineering from the East China University Of Science And Technology, China in 2015. He is currently pursuing the Ph.D. degree in mechatronic engineering at the Shanghai Jiao Tong University, China. His research interests include programming by demonstration and machine learning.

Xiaokang Shu received the Bachelor's degree from the School of Mechanical and Electronic Engineering at Wuhan University of Technology, Wuhan, China, in 2012. He is currently working toward the Ph.D. degree in the School of Mechanical Engineering at Shanghai Jiao Tong University, Shanghai, China. His research interests include mainly EEG signal processing and Brain–computer Interface (BCI) for stroke rehabilitation.

Kai Gui (S'—) received the bachelor's degree from the School of Mechanical Engineering and Automation, Southeast University, Nanjing, China, in 2013. He is currently pursuing the Ph.D. degree with the School of Mechanical Engineering, Shanghai Jiao Tong University, Shanghai, China. His research interests include robotic exoskeleton and human–machine systems.

Yulia Bezsudnova received the B.S. degree at school of General Physics and Molecular Electronics and M.S. degree at school of General Physics and Wave processes from the Moscow State University, Russian Federation in 2015 and 2017 respectively. She is currently working toward the Ph.D. degree in mechatronic engineering at the Shanghai Jiao Tong University, China. Her research interests include brain–computer interface and robotic exoskeleton.

Xinjun Sheng (M'11) received the B.Sc., M.Sc., and Ph.D. degrees in mechanical engineering from Shanghai Jiao Tong University, Shanghai, China, in 2000, 2003, and 2014, respectively. He was a Visiting Scientist with Concordia University, Montreal, QC, Canada, in 2012. He is currently an Associate Professor with the School of Mechanical Engineering, Shanghai Jiao Tong University. His current research interests include robotics and biomechatronics.

Dr. Sheng is a member of the IEEE Robotics and Automation Society, IEEE Engineering in Medicine and Biology Society, and IEEE Industrial Electronics Society.

Dingguo Zhang (M'07-SM'14) received the Bachelor's degree in electrical engineering from Jilin University, China, in 2000, the Master's degree in control engineering from the Harbin Institute of Technology, China, in 2002, and the Ph.D. degree from Nanyang Technological University, Singapore, in 2007. From 2006 to 2007, he was a Research Fellow at Nanyang Technological University. In 2008, he was a Postdoctoral Fellow at LIRMM of CNRS, France. He is currently an Associate Professor at the Robotics Institute, Shanghai Jiao Tong University, China. His research interests include human–machine systems, rehabilitation technologies, and biomechatronics.

Dr. Zhang is an IEEE senior member (EMBS, RAS, and SMC) and an IFESS lifetime member. He is a board member of IFESS, a youth commission member of ISBE. He serves in 3 technical committees of EMBS and SMC. He is an associate editor (or editorial board member) of 4 journals: IEEE Access, IEEE Trans. Human–Machine Systems, PLOS One, and Scientific Reports. He is a topic editor of Frontiers in Neuroscience. He is the recipient of the Delsys Prize 2011 (USA), and a nominee of the BCI Award 2015 (Austria).